IEEE Access
Multidisciplinary | Rapid Review | Open Access Journal

Received April 10, 2020, accepted April 26, 2020, date of publication June 2, 2020, date of current version June 17, 2020.

Digital Object Identifier 10.1109/ACCESS.2020.2999412

Continuous Fixed-Time Sliding Mode Attitude Controller Design for Rigid-Body Spacecraft

LEI WANG AND ZHUOYUE SONG
State Key Laboratory of Intelligent Control and Decision of Complex Systems, Beijing Institute of Technology, Beijing 100081, China
School of Automation, Beijing Institute of Technology, Beijing 100081, China

Corresponding author: Zhuoyue Song (szhuoyue@bit.edu.cn)

This work was supported in part by the U.S. Department of Commerce under Grant BS123456.

ABSTRACT Fast and high-precision attitude control for the rigid spacecraft is important for its broad applications in astronautics. In this paper, we address this problem via continuous nonsingular fixed-time sliding mode control approach. At first, by improving the adding power integral technique, a nonsingular nominal attitude controller is presented to achieve fixed-time convergence of the unperturbed attitude system, which underpins the basics for design of the sliding mode motion and surfaces for the subsequent proposed main results. Then, a fixed-time full-order sliding mode controller with an explicit bound of settling time is proposed to track the desire attitude even in the presence of external disturbances. However, this controller requires the angular acceleration signals which is usually unmeasurable. To this end, an integral sliding mode controller is further presented to achieve fixed-time attitude tracking without using any acceleration information. This proposed integral sliding mode controller can realize second-order sliding mode with rigorous proof of fixed-time convergence. Both the proposed fixed time full-order and integral sliding mode controller are inherent nonsingular and chattering-free. Numerical examples are illustrated to demonstrate the effectiveness of the results given herein in practical scenarios.

INDEX TERMS Attitude control, sliding mode control, fixed-time convergence.

I. INTRODUCTION

In the past decades, the attitude control of spacecraft has been paid attention widely from the control community for its broad applications in astronautics, such as deep space exploration, space-based interferometry and surveillance, etc. [1], [2]. However, high-precision rapid attitude controller design is still one of the most complicated and challenging problems. It is not only due to the inherent nonlinear and coupling characteristics in the attitude dynamics and kinematics, but also because there are the severe external disturbances which arise from gravity gradient, atmospheric drag, and magnetic effects, etc [3]–[5]. To this end, a great many researches on spacecraft attitude control have been done under various assumptions and scenarios [4]–[9].

Sliding mode control (SMC) is one of the most popular methods in attitude controller design for its strong robustness and computational simplicity in handling nonlinear control systems with disturbances [3], [10]–[12]. Particularly, finite-time stabilization is popular since it can provide faster convergence, higher control precision, and better anti-disturbance performance. To name a few, by resorting to terminal SMC (TSMC) method, the authors in [13]–[15] present the robust attitude controllers to achieve finite-time convergence at the cost of singularity in control signals. To eliminate this singularity, nonsingular TSMC (NTSMC) technique is further adopted in [16]–[18] to design finite-time attitude controllers without causing singularity. At the same time, the authors in [1], [19]–[21] present another class of nonsingular finite-time TSMC by switching from the terminal sliding manifold to a differential general sliding manifold. Nevertheless, it is worth mentioning that the settling time of finite-time stabilization is still dependent on the initial states, which means the convergence time is difficult to estimate when the initial states are unknown in prior.

Recently, fixed-time control method, in which the upper bound of settling time is independent of the initial states [22], is studied for the attitude control of rigid spacecraft under various assumptions and scenarios [23]–[30]. For instance, the NTSMC is extended in [28], [29] to the fixed-time attitude controller design of rigid spacecraft, and the authors in [30] further introduce a sinusoid function into the fixed-time

The associate editor coordinating the review of this manuscript and approving it for publication was Chao-Yang Chen.

NTSMC design and guarantee a fixed settling time. In [23]–[25], by using switching fixed-time sliding mode surface, robust fixed-time attitude controllers for rigid spacecraft is proposed based on quaternion or rotation matrix. Disturbance observer method and homogeneity theorem are utilized to design fixed-time attitude controllers for rigid spacecraft with actuator faults in [27] and flexible spacecraft in [26]. Reference [31] proposes a discontinuous controller via add a power integral technique to stabilize the attitude in fixed time.

Although fruitful results have been achieved in fixed-time attitude control problem in the above-mentioned literatures, there still remain some issues that need to be noticed. Note that the singularity is eliminated in the controllers [23]–[25] by switching fixed-time sliding mode surface, while the attitude tracking error can only converge to a region in fixed time. As for the NTSMC-based attitude controllers in [28]–[30], the convergence time in reaching phase is complicated to estimated. Another problem is the discontinuity in control action. Specifically, the discontinuous control torques required in [24], [30], [31] may lead to chattering phenomenon, which can damage the actuators and excite unmodeled high-frequency dynamics. In general, this problem could be eliminated through the saturation function (boundary layer method), which is suggested in [24], [29]. However, the cost is the degradation of the steady control accuracy, since the sliding mode function can only converge to the boundary layer in finite or fixed time. Although high-order sliding mode control and full-order sliding mode control are applied in [32], [33] to design finite-time continuous nonsingular attitude controller, to the best of authors' knowledge, there are still few works which can ensure fixed-time convergence and provide continuous control torques for the disturbed rigid spacecraft without using disturbance observers. Furthermore, feedback linearization or state transformation used in the controllers [24]–[27] brings heavy computation burden, since these controllers need real-time calculation of the complicated accurate compensation terms and the inverse of the Jacobian matrix. Therefore, it is interesting and necessary to design robust high-precision fixed-time attitude controllers without causing singularity or chattering.

In this paper, we study the fixed-time attitude tracking problem for the rigid-body spacecraft with unknown external disturbance. First, by improving traditional adding power integral technique (APIT), we first present a novel nominal attitude controller to construct the sliding mode motion for the main results. As full-order sliding mode control and super twisting algorithm (STA) can both generate continuous control action, we further propose fixed-time full-order sliding mode controller (FxFSMC) and fixed-time integral sliding mode controller (FxISMC) to ensure zero attitude tracking error in fixed time, where STA is chosen as the reaching law of FxISMC. Both FxFSMC and FxISMC are inherent nonsingular and chattering-free, since the singular term is avoided via improved APIT, and the control action generated by FxFSMC and FxISMC are continuous. The contributions are summarized as follows:

(1) The design of Lyapunov function and virtual velocity in APIT is improved in this paper to design a nonsingular fixed-time attitude controller for the unperturbed attitude system. Compared with the direct extension of traditional APIT to the fixed-time attitude controller [31], our improvements simplify the design procedure and reduce computational complexity of the controller.

(2) Via the idea of integral sliding mode and fixed-time STA technique, FxISMC is proposed to achieve fixed-time convergence without using any acceleration information. Moreover, the proposed FxISMC can realize second-order sliding mode $\dot{s} = s = 0$ and provide rigorous proof of fixed-time convergence for the attitude and angular velocity tracking error. While most existing integral sliding mode controllers, such as [27], [34], can only achieve first-order sliding mode $s = 0$.

(3) The proposed FxFSMC and FxISMC are designed based on attitude and angular velocity explicitly/directly, which simplifies controller structure and reduces computation compared with the controllers based on feedback linearization [24], [27].

Notation. $\boldsymbol{I}_3$ denotes 3×3 identity matrix. $\|\cdot\|$ denote Euclidean norm for vector or induced 2-norm for matrix, respectively. For $\boldsymbol{v} = [v_1, v_2, v_3]^T \in R^3$, $\boldsymbol{v}^\times \triangleq [0, -v_3, v_2; v_3, 0, -v_1; -v_2, v_1, 0]$, $\mathrm{diag}(\boldsymbol{v}) \triangleq [v_1, 0, 0; 0, v_2, 0; 0, 0, v_3]$. For $x \in \mathbb{R}$ and any constant p, the function $x \mapsto \lceil x \rfloor^p$ is defined as $\mathrm{sign}(x)|x|^p$, where $\mathrm{sign}(\cdot)$ is the signum function. Based on this definition, we can obtain that for any constants p and q, $\partial \lceil x \rfloor^p / \partial x = p|x|^{p-1}$, $\lceil x \rfloor^p \lceil x \rfloor^q = |x|^{p+q}$, $\lceil \lceil x \rfloor^p \rfloor^q = |x|^{pq}$. For $\boldsymbol{x} = [x_1, \cdots, x_n]^T \in \mathbb{R}^n$ and $p \in \mathbb{R}$, $|\boldsymbol{x}|^p \triangleq [|x_1|^p, \cdots, |x_n|^p]^T$. $\lceil \boldsymbol{x} \rfloor^p \triangleq [\lceil x_1 \rfloor^p, \cdots, \lceil x_n \rfloor^p]^T$. For a vector $\boldsymbol{x}$, $H(\boldsymbol{x}) = (1 + \boldsymbol{x}^T\boldsymbol{x})/4$.

II. PROBLEM FORMULATION

In this paper, the orientation of the rigid spacecraft with respect to the inertial frame is described in terms of the Modified Rodriguez Parameters (MRPs). The attitude kinematics and dynamics of the spacecraft are given by

$$\dot{\boldsymbol{\sigma}} = \boldsymbol{G}(\boldsymbol{\sigma})\boldsymbol{\omega}, \quad \boldsymbol{J}\dot{\boldsymbol{\omega}} = -\boldsymbol{\omega}^\times \boldsymbol{J}\boldsymbol{\omega} + \boldsymbol{u} + \boldsymbol{d} \tag{1}$$

where $\boldsymbol{\sigma} \in \mathbb{R}^3$ is MRPs of the rigid spacecraft, $\boldsymbol{\omega} \in \mathbb{R}^3$ is the angular velocity of the spacecraft with respect to the inertial frame expressed in the body frame, $\boldsymbol{J} \in \mathbb{R}^{3\times 3}$ and $\boldsymbol{u} = [u_1, u_2, u_3]^T \in \mathbb{R}^3$ are the inertia and the control torque of spacecraft, $\boldsymbol{d} = [d_1, d_2, d_3]^T \in \mathbb{R}^3$ is the unknown external disturbance vector satisfying Assumption 1, and $\boldsymbol{G}(\boldsymbol{\sigma}) = (1/2)[(1 - \boldsymbol{\sigma}^T\boldsymbol{\sigma})/2\boldsymbol{I}_3 + \boldsymbol{\sigma}^\times + \boldsymbol{\sigma}\boldsymbol{\sigma}^T]$. The matrix $\boldsymbol{G}(\boldsymbol{\sigma})$ has the following properties [20],

$$\begin{aligned} &\boldsymbol{\sigma}^T\boldsymbol{G}(\boldsymbol{\sigma})\boldsymbol{\omega} = H(\boldsymbol{\sigma})\boldsymbol{\sigma}^T\boldsymbol{\omega}, \\ &\boldsymbol{G}(\boldsymbol{\sigma})\boldsymbol{G}^T(\boldsymbol{\sigma}) = \boldsymbol{G}^T(\boldsymbol{\sigma})\boldsymbol{G}(\boldsymbol{\sigma}) = H^2(\boldsymbol{\sigma})\boldsymbol{I}_3 \end{aligned} \tag{2}$$

where $H(\boldsymbol{\sigma}) \geqslant 1/4$.

Assumption 1 ([32], [33]): The external disturbances satisfy $|\dot{d}_i| \leqslant L < \infty$, $i = 1, 2, 3$, where L is a known constant.

The desired trajectory $\boldsymbol{\sigma_r}$ is constructed to avoid the kinematic singularity associated with the MRPs and $\boldsymbol{\omega_r}, \dot{\boldsymbol{\omega}}_{\boldsymbol{r}}$ are assumed to be bounded. In what follows, to solve the attitude tracking problem, as in [31], we define $\boldsymbol{e} = [e_1, e_2, e_3]^T$ as the relative attitude error between the actual and desired attitudes, where

$$\boldsymbol{e} = \boldsymbol{\sigma} \otimes \boldsymbol{\sigma_r}^{-1} = \frac{\boldsymbol{\sigma_r}(\boldsymbol{\sigma}^T\boldsymbol{\sigma} - 1) + \boldsymbol{\sigma}(1 - \boldsymbol{\sigma_r}^T\boldsymbol{\sigma_r}) + 2\boldsymbol{\sigma}^\times\boldsymbol{\sigma_r}}{1 + \boldsymbol{\sigma_r}^T\boldsymbol{\sigma_r}\boldsymbol{\sigma}\boldsymbol{\sigma}^T + 2\boldsymbol{\sigma_r}^T\boldsymbol{\sigma}}$$

Define $\boldsymbol{v} = [v_1, v_2, v_3]^T = \boldsymbol{\omega} - \boldsymbol{R_d^b}\boldsymbol{\omega_r} \in \mathbb{R}^3$ as the as the relative angular velocity error, where $\boldsymbol{R_d^b}$ is the rotation matrix from the desired reference frame to the body reference frame. $\boldsymbol{R_d^b}$ is an orthogonal rotation matrix given by $\boldsymbol{R_d^b} = \boldsymbol{I}_3 - 4((1-\boldsymbol{e}^T\boldsymbol{e})/(1+\boldsymbol{e}^T\boldsymbol{e})^2)\boldsymbol{e}^\times + 8(\boldsymbol{e}^\times)^2/(1+\boldsymbol{e}^T\boldsymbol{e})^2$. Then, the relative kinematic and dynamic equations are represented as follows:

$$\begin{cases} \dot{\boldsymbol{e}} = \boldsymbol{G}(\boldsymbol{e})\boldsymbol{v} \\ \boldsymbol{J}\dot{\boldsymbol{v}} = -\boldsymbol{\omega}^\times\boldsymbol{J}\boldsymbol{\omega} + \boldsymbol{u} - \boldsymbol{J}\boldsymbol{R_d^b}\dot{\boldsymbol{\omega}}_{\boldsymbol{r}} + \boldsymbol{J}\boldsymbol{v}^\times\boldsymbol{R_d^b}\boldsymbol{\omega_r} + \boldsymbol{d} \end{cases} \tag{3}$$

The control objective of this paper is to design a fixed time attitude tracking control law for the spacecraft in (1) such that the desired attitude can be tracked in fixed time in the presence of unknown disturbances. Specifically, $\boldsymbol{e}$ and $\boldsymbol{v}$ converge to zero in fixed time, i.e. the settling time is bounded by a value that is independent with any initial states.

The next several lemmas are provided here to streamline the main results in the next section.

Lemma 1 ([28]): Consider the nonlinear system

$$\dot{\boldsymbol{x}} = \boldsymbol{f}(\boldsymbol{x}, t), \quad \boldsymbol{x} = \boldsymbol{x_0}, \boldsymbol{f}(\boldsymbol{0}) = \boldsymbol{0},$$

where $\boldsymbol{x} \in \mathbb{R}^n$, and $\boldsymbol{f} : \mathbb{R}^n \to \mathbb{R}^n$. Suppose that there exists a continuous positive-definite function $V : \mathbb{R}^n \to \mathbb{R}$ such that $\dot{V} \leqslant -\alpha V^p - \beta V^q$, where $\alpha > 0$, $\beta > 0$, $p \in (0, 1)$, $q > 1$. Then, $\forall \boldsymbol{x}(0) \in \mathbb{R}^n$, the state $\boldsymbol{x}$ converges to zero in fixed time T, and T satisfies $T \leqslant \frac{1}{\alpha(1-p)} + \frac{1}{\beta(q-1)}$.

Lemma 2 ([35]): Consider the following dynamic system (4) with state $x, y \in \mathbb{R}$ and bounded disturbance $|d| < L$,

$$\begin{aligned} \dot{x} &= -k_1(\lceil x \rfloor^{1/2} + \mu\lceil x \rfloor^{3/2}) + y \\ \dot{y} &= -k_2(\frac{1}{2}\lceil x \rfloor^{1/2} + 2\mu x + \frac{3}{2}\mu^2\lceil x \rfloor^2) + d. \end{aligned} \tag{4}$$

If the control parameters satisfy $k_1 > 2\sqrt{L}$, $k_2 > 2L$, and $\mu > 0$, then the states x, y will converge to zero in fixed time.

Lemma 3 ([36]): If $0 < p < 1$, $\forall x, y \in \mathbb{R}$, we have $|\lceil x \rfloor^p - \lceil y \rfloor^p| \leqslant 2^{1-p}|x - y|^p$.

Lemma 4 ([36]): If $c, d > 0$ and $\gamma > 0$, $\forall x, y \in \mathbb{R}$, we have $|x|^c|y|^d \leqslant \frac{c}{c+d}\gamma|x|^{c+d} + \frac{d}{c+d}\gamma^{-\frac{c}{d}}|y|^{c+d}$, the equality holds if and only if $\gamma^{(1+c/d)/(c+d)}|x| = |y|$.

Lemma 5 ([2]): For any $x_i \in \mathbb{R}$, $i = 1, \cdots, n$, and $p \in (0, 1]$, $\left(\sum_{i=1}^n |x_i|\right)^p \leqslant \sum_{i=1}^n |x_i|^p \leqslant n^{1-p}\left(\sum_{i=1}^n |x_i|\right)^p$.

Lemma 6 ([37]): For any $x_i \in \mathbb{R}$, $i = 1, \cdots, n$, and $q > 1$, $\sum_{i=1}^n |x_i|^q \leqslant \left(\sum_{i=1}^n |x_i|\right)^q \leqslant n^{q-1}\sum_{i=1}^n |x_i|^q$.

III. MAIN RESULTS

A. NOMINAL ATTITUDE CONTROLLER DESIGN

In this subsection, we will present a nominal continuous nonsingular fixed-time attitude controller via improved APIT for the nominal attitude dynamics (i.e. $\boldsymbol{d} = \boldsymbol{0}$ in (1)). Note that the nominal closed-loop system dynamics with this controller underpins the sliding mode surface design of the subsequent controllers FxFSMC and FxISMC.

The nominal fixed-time attitude controller $\boldsymbol{u_n}$ for the spacecraft system (1) with $\boldsymbol{d} = \boldsymbol{0}$ is designed as

$$\begin{aligned} \boldsymbol{u_n} = {} & \boldsymbol{J}\boldsymbol{R_d^b}\dot{\boldsymbol{\omega}}_{\boldsymbol{r}} - \boldsymbol{J}\boldsymbol{v}^\times\boldsymbol{R_d^b}\boldsymbol{\omega_r} + \boldsymbol{\omega}^\times\boldsymbol{J}\boldsymbol{\omega} \\ & - \boldsymbol{C}_3\boldsymbol{H}(\boldsymbol{e})\boldsymbol{J}\lceil\boldsymbol{\xi}\rfloor^{2p-1} - \boldsymbol{C}_4\boldsymbol{H}(\boldsymbol{e})\boldsymbol{J}\lceil\boldsymbol{\xi}\rfloor^{p+q-1} \end{aligned} \tag{5}$$

where $p \in (1/2, 1)$, $q \in (1, \infty)$,

$$\boldsymbol{\xi} = \lceil\boldsymbol{v}\rfloor^{1/p} + c_1^{1/p}\boldsymbol{e} + c_2^{1/p}\lceil\boldsymbol{e}\rfloor^{q/p}, \tag{6}$$

$\boldsymbol{C}_j = \mathrm{diag}([c_{j1}, c_{j2}, c_{j3}])$, $j = 3, 4$,

$$\begin{aligned} c_1 &= \frac{2^{1-p}\mu_1}{(1+p)} + 3^{3/2}2^{1-2p}\lambda_1 + \frac{2^{-p}3^{2-p}\lambda_2}{1+p} \\ c_2 &= \frac{4^{(q-1)/(p+q)}}{(1+p)3^{(1-q)/2}2^{p-1}}\mu_2 + \frac{3^{(q+1)/2}qC_{p,q}\lambda_3}{(p+q)(1+p)2^{p-1}} \\ c_{3i} &= 2^{1-p}\mu_1 + (1+p)\frac{2^{1-2p}3^{1/2}}{\lambda_1} + \frac{2^{-p}3c_1^2m^2(e_i)}{\lambda_2} \\ &\quad + 2^{2-2p}3m(e_i) \\ c_{4i} &= \frac{4^{(q-1)/(p+q)}}{2^{p-1}}\mu_2 + \frac{\left(3pc_2m(e_i)\right)^{q/p+1}}{2^{p-1}(p+q)\lambda_3^{q/p}} \end{aligned} \tag{7}$$

$m(e_i) = \left(c_1^{1/p} + c_2^{1/p}q/p|e_i|^{q/p-1}\right)$, $i = 1, 2, 3$, $\lambda_1, \lambda_2, \lambda_3$ are arbitrary positive constants, μ_1, μ_2 are positive controller parameters, and

$$C_{p,q} = \begin{cases} 1, & p+q \leq 2, \\ 3^{1-(p+q)/2}, & p+q > 2. \end{cases}$$

Then, it follows that with the proposed nominal controller (5), the nominal closed-loop attitude system becomes

$$\begin{cases} \dot{\boldsymbol{e}} = \boldsymbol{G}(\boldsymbol{e})\boldsymbol{v}, \\ \dot{\boldsymbol{v}} = -\boldsymbol{C}_3\,\boldsymbol{H}(\boldsymbol{e})\lceil\boldsymbol{\xi}\rfloor^{2p-1} - \boldsymbol{C}_4\,\boldsymbol{H}(\boldsymbol{e})\lceil\boldsymbol{\xi}\rfloor^{p+q-1}. \end{cases} \tag{8}$$

The next lemma shows that the states $\boldsymbol{e}, \boldsymbol{v}$ of the nominal closed-loop system (8) converge to zero in fixed time.

Lemma 7: Consider the spacecraft system (1) with $\boldsymbol{d} = \boldsymbol{0}$, if the control torque is chosen as $\boldsymbol{u_n}$ in (5) with proper parameters satisfying (7), then the desired attitude can be tracked in fixed time, and the settling time T_1 is bounded by

$$T_1 \leq \frac{4(1+p)}{\mu_1(1-p)} + \frac{4(1+p)}{\mu_2(q-1)}. \tag{9}$$

Proof: First, we define the virtual angular velocity input $\boldsymbol{v}^*$ as

$$\boldsymbol{v}^* = -\lceil c_1^{1/p}\boldsymbol{e} + c_2^{1/p}\lceil\boldsymbol{e}\rfloor^{q/p}\rfloor^p, \tag{10}$$

and $\boldsymbol{\xi} = [\xi_1, \xi_2, \xi_3]^T$ represents the auxiliary velocity tracking error

$$\boldsymbol{\xi} = \lceil\boldsymbol{v}\rfloor^{1/p} - \lceil\boldsymbol{v}^*\rfloor^{1/p}. \tag{11}$$

Note that the elements of $\boldsymbol{\xi}$ in (6), $\boldsymbol{v}^*$ in (10) and $\dot{\boldsymbol{v}}$ in (8) are

$$\begin{aligned}\dot{v}_i &= -c_{3i}H\lceil\xi_i\rfloor^{2p-1} - c_{4i}H\lceil\xi_i\rfloor^{p+q-1},\\ v_i^* &= -\lceil c_1^{1/p}e_i + c_2^{1/p}\lceil e_i\rfloor^{q/p}\rfloor^p,\\ \xi_i &= \lceil v_i\rfloor^{1/p} - \lceil v_i^*\rfloor^{1/p}\\ &= \lceil v_i\rfloor^{1/p} + c_1^{1/p}e_i + c_2^{1/p}\lceil e_i\rfloor^{q/p}, \quad i = 1, 2, 3.\end{aligned}$$

where H is shortened for $H(\boldsymbol{e})$.

Step 1 (The definition of the Lyapunov function): Choose the following Lyapunov candidate

$$V = V_0 + \sum_{i=1}^{3} V_i \tag{12}$$

where

$$V_0 = \left(\boldsymbol{e}^T\boldsymbol{e}\right)^{(1+p)/2} \tag{13}$$

$$V_i = 2^{p-1}\int_{v_i^*}^{v_i} \lceil y\rfloor^{1/p} - \lceil v_i^*\rfloor^{1/p}\mathrm{d}y, \quad i = 1, 2, 3. \tag{14}$$

The functions V_i, $i = 1, 2, 3$ are positive definite and radially unbounded (see the proof in the Appendix).

Step 2 (The calculation of $\dot{V}_0$): Taking the derivative of V_0, we have

$$\begin{aligned}\dot{V}_0 &= (1+p)\left(\boldsymbol{e}^T\boldsymbol{e}\right)^{(p-1)/2}\boldsymbol{e}^T\dot{\boldsymbol{e}}\\ &= (1+p)HV_0^{(p-1)/(p+1)}\boldsymbol{e}^T\boldsymbol{v}\\ &= (1+p)HV_0^{(p-1)/(p+1)}\sum\nolimits_{i=1}^{3} e_iv_i\end{aligned} \tag{15}$$

Note that for $i = 1, 2, 3$,

$$\begin{aligned}e_iv_i &= e_iv_i^* + e_i(v_i - v_i^*)\\ &= -e_i\lceil c_1^{1/p}e_i + c_2^{1/p}\lceil e_i\rfloor^{q/p}\rfloor^p + e_i(v_i - v_i^*)\\ &= -|e_i|\left(c_1^{1/p}|e_i| + c_2^{1/p}|e_i|^{q/p}\right)^p + e_i(v_i - v_i^*)\\ &= -\underbrace{\left(c_1^{1/p}|e_i|^{1+1/p} + c_2^{1/p}|e_i|^{(1+q)/p}\right)^p}_{\text{via Lemma 5}} + e_i\underbrace{(v_i - v_i^*)}_{\text{via Lemma 3}}\\ &\le -c_12^{p-1}|e_i|^{1+p} - c_22^{p-1}|e_i|^{1+q} + 2^{1-p}|e_i||\xi_i|^p\end{aligned}$$

It then follows from (15) that

$$\begin{aligned}\dot{V}_0 \le\ & -c_1(1+p)2^{p-1}HV_0^{(p-1)/(p+1)}\sum_{i=1}^{3}|e_i|^{1+p}\\ & - c_2(1+p)2^{p-1}HV_0^{(p-1)/(p+1)}\sum_{i=1}^{3}|e_i|^{1+q}\\ & + (1+p)2^{1-p}HV_0^{(p-1)/(p+1)}\sum_{i=1}^{3}|e_i||\xi_i|^p\end{aligned} \tag{16}$$

Noting $(1+p)/2 \in (0, 1)$, then via Lemma 5,

$$\begin{aligned}\sum_{i=1}^{3}|e_i|^{1+p} &= \sum_{i=1}^{3}|e_i|^{2*(1+p)/2}\\ &\ge \left(\sum_{i=1}^{3}|e_i|^2\right)^{(1+p)/2}\\ &= V_0\end{aligned} \tag{17}$$

Similarly, since $(1+q)/2 > 1$, via Lemma 6,

$$\begin{aligned}\sum_{i=1}^{3}|e_i|^{1+q} &= \sum_{i=1}^{3}|e_i|^{2*(1+q)/2}\\ &\ge 3^{1-(1+q)/2}\left(\sum_{i=1}^{3}|e_i|^2\right)^{(1+q)/2}\\ &= 3^{(1-q)/2}V_0^{(1+q)/(1+p)}\end{aligned} \tag{18}$$

Also, via Lemma 5, we have

$$|e_i| \le \sum_{i=1}^{3}|e_i| \le 3^{1/2}\left(\sum_{i=1}^{3}|e_i|^2\right)^{1/2} \le 3^{1/2}V_0^{1/(1+p)}$$

Then, it follows that

$$\begin{aligned}& V_0^{(p-1)/(p+1)}\sum_{i=1}^{3}|e_i||\xi_i|^p\\ &\le 3^{1/2}\sum_{i=1}^{3}V_0^{p/(1+p)}|\xi_i|^p\\ &\le 3^{1/2}\sum_{i=1}^{3}\left(V_0^{1/(1+p)}\right)^p|\xi_i|^p \ \text{(via Lemma 5)}\\ &\le \frac{3^{1/2}\lambda_1}{2}\sum_{i=1}^{3}V_0^{2p/(1+p)} + \frac{3^{1/2}}{2\lambda_1}\sum_{i=1}^{3}|\xi_i|^{2p}\\ &= \frac{3^{3/2}\lambda_1}{2}V_0^{2p/(1+p)} + \frac{3^{1/2}}{2\lambda_1}\sum_{i=1}^{3}|\xi_i|^{2p}\end{aligned} \tag{19}$$

Substituting (17), (18), and (19) into (16), we can obtain

$$\begin{aligned}\dot{V}_0 \le\ & -(1+p)\left(2^{p-1}c_1 - 3^{3/2}2^{-p}\lambda_1\right)HV_0^{2p/(p+1)}\\ & - (1+p)2^{p-1}3^{(1-q)/2}c_2HV_0^{(p+q)/(p+1)}\\ & + (1+p)2^{-p}\frac{3^{1/2}}{\lambda_1}H\sum_{i=1}^{3}|\xi_i|^{2p}\end{aligned} \tag{20}$$

Step 3 (The calculation of $\sum_{i=1}3\dot{V}_i$): Taking the derivative of V_i, $i = 1, 2, 3$, we have

$$\begin{aligned}\dot{V}_i &= 2^{p-1}\xi_i\dot{v}_i - 2^{p-1}\int_{v_i^*}^{v_i}\frac{\partial}{\partial t}\left(\lceil v_i^*\rfloor^{1/p}\right)\mathrm{d}y\\ &\le 2^{p-1}\xi_i\dot{v}_i + 2^{p-1}\left|\frac{\partial}{\partial t}\left(\lceil v_i^*\rfloor^{1/p}\right)\right||v_i - v_i^*|\\ &\le 2^{p-1}\xi_i\dot{v}_i + \left|\frac{\partial}{\partial t}\left(\lceil v_i^*\rfloor^{1/p}\right)\right||\xi_i|^p\end{aligned} \tag{21}$$

Noting that

$$\frac{\partial}{\partial t}\left(\lceil v_i^*\rfloor^{1/p}\right) = \frac{\partial}{\partial e_i}\left(c_1^{1/p}e_i + c_2^{1/p}\lceil e_i\rfloor^{q/p}\right)\dot{e}_i$$

$$= \left(c_1^{1/p} + c_2^{1/p} q/p |e_i|^{q/p-1}\right) \dot{e}_i$$
$$= m(e_i)\dot{e}_i \tag{22}$$

where $m(e_i) = \left(c_1^{1/p} + c_2^{1/p} q/p |e_i|^{q/p-1}\right)$.

Also via Lemma 6,

$$||\dot{\boldsymbol{e}}||^2 = \boldsymbol{v}^T \boldsymbol{G}^T \boldsymbol{G} \boldsymbol{v} = H^2 \sum_{j=1}^{3} |v_j|^2 \leqslant H^2 \left(\sum_{j=1}^{3} |v_j|\right)^2.$$

Hence, we have

$$\begin{aligned}
|\dot{e}_i| &\leqslant \|\dot{\boldsymbol{e}}\| \leq H \sum_{j=1}^{3} |v_j| \\
&\leq H \sum_{j=1}^{3} \left(|v_j^*| + |v_j - v_j^*|\right) \\
&\leq H \sum_{j=1}^{3} \left(\left|c_1^{1/p} e_j + c_2^{1/p} \lceil e_j \rfloor^{q/p}\right|^p + 2^{1-p} |\xi_j|^p\right) \\
&= H \sum_{j=1}^{3} \Big(\underbrace{\left(c_1^{1/p}|e_j| + c_2^{1/p}|e_j|^{q/p}\right)^p}_{\text{via Lemma 5}} + 2^{1-p}|\xi_j|^p\Big) \\
&\leq H \sum_{j=1}^{3} \left(c_1 |e_j|^p + c_2 |e_j|^q + 2^{1-p}|\xi_j|^p\right).
\end{aligned} \tag{23}$$

Substituting (22) and (23) into (21) results in

$$\begin{aligned}
\dot{V}_i &\leq 2^{p-1}\xi_i \dot{v}_i + \left|\frac{\partial}{\partial t}\left(\lceil v_i^* \rfloor^{1/p}\right)\right| |\xi_i|^p \\
&\leq 2^{p-1}\xi_i \dot{v}_i + m(e_i)|\dot{e}_i||\xi_i|^p \\
&\leq 2^{p-1}\xi_i \dot{v}_i + m(e_i) H |\xi_i|^p \\
&\quad \times \sum_{j=1}^{3} \left(c_1 |e_j|^p + c_2 |e_j|^q + 2^{1-p}|\xi_j|^{1/p}\right)
\end{aligned} \tag{24}$$

Via Lemma 4, we have

$$\begin{aligned}
|e_j|^p |\xi_i|^p &\leq \frac{\lambda_2}{2c_1 m(e_i)} |e_j|^{2p} + \frac{c_1 m(e_i)}{2\lambda_2} |\xi_i|^{2p} \\
|e_j|^q |\xi_i|^p &\leq \frac{q}{p+q} \frac{\lambda_3}{c_2 m(e_i)} |e_j|^{p+q} \\
&\quad + \frac{p}{p+q} \left(\frac{c_2 m(e_i)}{\lambda_3}\right)^{q/p} |\xi_i|^{p+q} \\
|\xi_j|^p |\xi_i|^p &\leq 1/2 |\xi_j|^{2p} + 1/2 |\xi_i|^{2p}
\end{aligned} \tag{25}$$

Since $p \in (0, 1)$, it follows from Lemma 5 that

$$\sum_{i=1}^{3} |e_i|^{2p} \leq 3^{1-p} \Big(\sum_{i=1}^{3} |e_i|^2\Big)^p = 3^{1-p} V_0^{2p/(1+p)} \tag{26}$$

If $p + q \leq 2$, then by Lemma 5,

$$\sum_{i=1}^{3} |e_i|^{p+q} \leq 3^{1-(p+q)/2} V_0^{(q+p)/(1+p)} \tag{27}$$

Otherwise $p + q > 2$, via Lemma 6,

$$\sum_{i=1}^{3} |e_i|^{p+q} \leq \Big(\sum_{i=1}^{3} |e_i|^2\Big)^{(p+q)/2} = V_0^{(q+p)/(1+p)} \tag{28}$$

Hence, for both the cases of (27) and (28), we have

$$\sum_{i=1}^{3} |e_i|^{p+q} \leq C_{p,q} V_0^{(q+p)/(1+p)} \tag{29}$$

Then, it follows from (24), (25), (26) and (29) that

$$\begin{aligned}
\sum_{i=1}^{3} \dot{V}_i &\leq 2^{p-1} \sum_{i=1} \xi_i \dot{v}_i + H \sum_{i=1}^{3} \sum_{j=1}^{3} \Big(\frac{\lambda_2}{2} |e_j|^{2p} \\
&\quad + \frac{c_1^2 m^2(e_i)}{2\lambda_2} |\xi_i|^{2p} + \frac{q\lambda_3}{p+q} |e_j|^{p+q} \\
&\quad + \frac{p}{p+q} \frac{\left(c_2 m(e_i)\right)^{q/p+1}}{(\lambda_3)^{q/p}} |\xi_i|^{p+q} \\
&\quad + m(e_i) 2^{1-p} 1/2 |\xi_j|^{2p} + 2^{1-p} 1/2 m(e_i) |\xi_i|^{2p}\Big) \\
&\leq 2^{p-1} \sum_{i=1} \xi_i \dot{v}_i + \frac{3qC_{p,q}\lambda_3}{p+q} H V_0^{(p+q)/(1+p)} \\
&\quad + \frac{3^{2-p}\lambda_2}{2} H V_0^{2p/(1+p)} + H \sum_{i=1}^{3} \Big(\frac{3c_1^2 m^2(e_i)}{2\lambda_2} |\xi_i|^{2p} \\
&\quad + \frac{3p\left(c_2 m(e_i)\right)^{q/p+1}}{(p+q)(\lambda_3)^{q/p}} |\xi_i|^{p+q} + 2^{1-p} 3 m(e_i) |\xi_i|^{2p}\Big)
\end{aligned} \tag{30}$$

Step 4 (Proving fixed-time convergence of the nominal system (8)): Combining (20) with (30) and substituting $\dot{v}_i = -c_{3i} H \lceil \xi_i \rfloor^{2p-1} - c_{4i} H \lceil \xi_i \rfloor^{p+q-1}$, $i = 1, 2, 3$, we can get

$$\begin{aligned}
\dot{V} &= \dot{V}_0 + \sum_{i=1}^{3} \dot{V}_i \\
&\leq -a_1 H V_0^{2p/(p+1)} - a_2 H V_0^{(p+q)/(p+1)} \\
&\quad - H \sum_{i=1}^{3} a_{3i} |\xi_i|^{2p} - H \sum_{i=1}^{3} a_{4i} |\xi_i|^{q+p}
\end{aligned} \tag{31}$$

where

$$\begin{aligned}
a_1 &= (1+p)2^{p-1} c_1 - (1+p) 3^{3/2} 2^{-p} \lambda_1 - \frac{3^{2-p}\lambda_2}{2} \\
a_2 &= (1+p)2^{p-1} 3^{(1-q)/2} c_2 - \frac{3qC_{p,q}\lambda_3}{p+q} \\
a_{3i} &= 2^{p-1} c_{3i} - (1+p)\frac{2^{-p} 3^{1/2}}{\lambda_1} - \frac{3c_1^2 m^2(e_i)}{2\lambda_2} \\
&\quad - 3m(e_i) 2^{1-p}, \quad i = 1, 2, 3 \\
a_{4i} &= 2^{p-1} c_{4i} - \frac{3p}{p+q} \frac{\left(c_2 m(e_i)\right)^{q/p+1}}{\lambda_3^{q/p}}, \quad i = 1, 2, 3
\end{aligned} \tag{32}$$

Also, via Lemma 5 and 6, we have

$$V_0^{2p/(p+1)} + \sum_{i=1}^{3} |\xi_i|^{2p}$$

$$\geq \Big(V_0 + \sum_{i=1}^{3} |\xi_i|^{p+1}\Big)^{2p/(p+1)}$$
$$\times V_0^{(p+q)/(p+1)} + \sum_{i=1}^{3} |\xi_i|^{q+p}$$
$$\geq 4^{(1-q)/(1+p)}\Big(V_0 + \sum_{i=1}^{3} |\xi_i|^{p+1}\Big)^{(p+q)/(p+1)}$$
$$V_i \leqslant 2^{p-1}\big|\lceil v_i\rfloor^{1/p} - \lceil v_i^*\rfloor^{1/p}\big|\big|v_i - v_i^*\big| \leqslant |\xi_i|^{1+p}. \quad (33)$$

Then, substituting these inequalities in (33) into (31) yields

$$\dot{V} \leq -\mu_1 H\left(V_0^{2p/(p+1)} + \sum_{i=1}^{3} |\xi_i|^{2p}\right)$$
$$- 4^{(q-1)/(1+p)}\mu_2 H\left(V_0^{(p+q)/(p+1)} + \sum_{i=1}^{3} |\xi_i|^{q+p}\right)$$
$$\leq -\mu_1 H\Big(V_0 + \sum_{i=1}^{3} |\xi_i|^{p+1}\Big)^{2p/(p+1)}$$
$$- \mu_2 H\Big(V_0 + \sum_{i=1}^{3} |\xi_i|^{p+1}\Big)^{(p+q)/(p+1)}$$
$$\leq -\mu_1 H V^{r_1} - \mu_2 H V^{r_2} \quad (34)$$

where $r_1 = 2p/(p+1) < 1$, $r_2 = (p+q)/(p+1) > 1$. Noting that $H = H(\boldsymbol{e}) \geq 1/4$, it follows that

$$\dot{V} \leq -\frac{\mu_1}{4} V^{r_1} - \frac{\mu_2}{4} V^{r_2} \quad (35)$$

Via Lemma 1, we can conclude that $\forall \boldsymbol{e}(0)$, $\boldsymbol{\xi}(0)$, the states $\boldsymbol{e}$ and $\boldsymbol{\xi}$ converge to zero in fixed time T_1, and T_1 satisfies

$$T_1 \leq \frac{4}{\mu_1(1-r_1)} + \frac{4}{\mu_2(r_2-1)} = \frac{4(1+p)}{\mu_1(1-p)} + \frac{4(1+p)}{\mu_2(q-1)}$$

Noting that $\boldsymbol{e} = \boldsymbol{0}$ implies $\boldsymbol{v}^* = \boldsymbol{0}$ and $\boldsymbol{\xi} = \lceil \boldsymbol{v}\rfloor^{1/p}$. Hence $\boldsymbol{v}$ also converges to zero in fixed time T_1. ■

Remark 1: Although the traditional adding a power integrator technique (APIT) is already studied in attitude controller designs [2], [5], [16], [31] to achieve finite-time and fixed-time convergence, in this paper, we improve the design of Lyapunov function V_0, V_i, $i = 1, 2, 3$ (see (13) and (14)) in APIT and simplifies the derivation of controller, especially the coupling term $\partial/\partial t V_i$, $i = 1, 2, 3$. Moreover, compared with the direct extension of APIT to fixed-time attitude control in [31], we further improve the form of virtual angular velocity input $\boldsymbol{v}^*$ in (6) to reduce real-time calculation burden of the bound of partial derivative $m(e_i) = |\partial/\partial e_i \lceil v_i^*\rfloor^{1/p}|$, $i = 1, 2, 3$.

Remark 2: As can be seen from (9), large μ_1 and μ_2 will accelerate the convergence. Besides, decreasing p or increasing q can improve the maximum settling time. To this end, in practice, the following parameter selection procedure is suggested: (a) choosing the parameters $p \in (0, 1)$, $q \in (1, \infty)$, μ_1 and μ_2 according the desired convergence settling time, (b) minimizing $\max\{c_1, c_2, c_{3i}, c_{4i}, i = 1, 2, 3\}$ in feasible zone $\{\lambda_k > 0, k = 1, 2, 3\}$ such that the conditions (7) with the assumption $m(e_i) = c_1^{1/p}$ are satisfied.

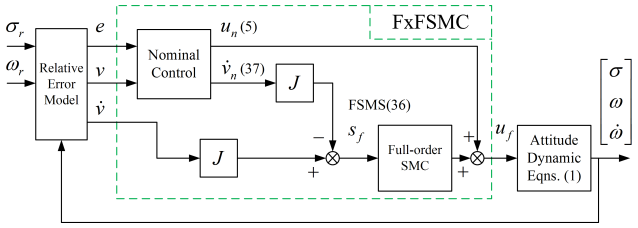

FIGURE 1. Block diagram of closed-loop attitude system with FxFSMC.

B. FULL-ORDER SLIDING MODE CONTROLLER DESIGN

In this subsection, the continuous fixed-time full-order sliding mode controller (FxFSMC) is presented to address the attitude tracking problem in the presence of disturbance $\boldsymbol{d}$ under Assumption 1.

The block diagram of our FxFSMC is given in Fig. 1, where the full-order sliding mode surface (FSMS) $\boldsymbol{s_f}$ is designed as the derivative of the angular momentum tracking error between $\boldsymbol{Jv}$ and $\boldsymbol{Jv_n}$,

$$\boldsymbol{s_f} = \boldsymbol{J}\dot{\boldsymbol{v}} - \boldsymbol{J}\dot{\boldsymbol{v}}_{\boldsymbol{n}} \quad (36)$$

where $\boldsymbol{v_n}$ is the nominal angular velocity input defined as

$$\dot{\boldsymbol{v}}_{\boldsymbol{n}} = -H(\boldsymbol{e})\boldsymbol{a}(\boldsymbol{e}, \boldsymbol{\xi}), \quad \boldsymbol{v_n}(0) = \boldsymbol{v}(0)$$
$$\boldsymbol{a}(\boldsymbol{e}, \boldsymbol{\xi}) = -\boldsymbol{c}_3\lceil\boldsymbol{\xi}\rfloor^{2p-1} - \boldsymbol{c}_4\lceil\boldsymbol{\xi}\rfloor^{p+q-1} \quad (37)$$

Note that the FSMS in (36) is designed to guarantee the system dynamic in (first-order) sliding mode $\boldsymbol{s_f} = \boldsymbol{0}$ is equivalent to the nominal closed-loop system (8). Then, the following full-order sliding mode attitude controller $\boldsymbol{u_f}$ is presented to drive the states onto the FSMS.

$$\begin{cases} \boldsymbol{u_f} = \boldsymbol{u_n} + \boldsymbol{z_f}, \\ \dot{\boldsymbol{z}}_{\boldsymbol{f}} = -k_1\lceil\boldsymbol{s_f}\rfloor^{q_1} - k_2\lceil\boldsymbol{s_f}\rfloor^{q_2} - k_3\lceil\boldsymbol{s_f}\rfloor^{0} \end{cases} \quad (38)$$

where $\boldsymbol{u_n}$ is defined in (5).

Theorem 1: For the spacecraft attitude control system in (1) with Assumptions 1 satisfied, suppose that the controller is designed as (38) and the FSMS is designed as (36). If the control parameters satisfy $k_1 > 0$, $k_2 > 0$, $k_3 > L$, $q_1 \in (0, 1)$, $q_2 \in (1, \infty)$, then the FSMS $\boldsymbol{s_f}$ converges to zero in fixed time, and the settling time T_2 is bounded by

$$T_2 \leqslant \frac{2}{2^{1/2+q_1/2}k_1(1-q_1)} + \frac{2}{2^{1/2+q_2/2}k_2(q_2-1)}. \quad (39)$$

Furthermore, and state errors $\boldsymbol{e}$ and $\boldsymbol{v}$ will converge to zero in fixed time $T_1 + T_2$, where T_1 is bounded by (9).

Proof: Let $\boldsymbol{s_f} = [s_{f1}, s_{f2}, s_{f3}]^T$, $\boldsymbol{z_f} = [z_{f1}, z_{f2}, z_{f3}]^T$. Choose the following Lyapunov function candidate

$$V_f = \frac{1}{2}\boldsymbol{s_f}^T\boldsymbol{s_f} = \sum_{i=1}^{3} s_{fi}^T s_{fi} \quad (40)$$

Taking the derivative of V_f, we have

$$\dot{V}_f = \sum_{i=1}^{3} s_{fi}\dot{s}_{fi} \tag{41}$$

Substituting (38) and (5) into (3), we can obtain

$$\boldsymbol{J}\dot{\boldsymbol{v}} = -H(\boldsymbol{e})\boldsymbol{J}\boldsymbol{a}(\boldsymbol{e},\boldsymbol{\xi}) + \boldsymbol{z_f} + \boldsymbol{d}$$

Then the FSMS $\boldsymbol{s_f}$ becomes

$$\boldsymbol{s_f} = \boldsymbol{J}\dot{\boldsymbol{v}} - \boldsymbol{J}\dot{\boldsymbol{v}}_{\boldsymbol{n}} = \boldsymbol{z_f} + \boldsymbol{d}$$

Hence, it follows from (41) that

$$\begin{aligned}
\dot{V}_f &= \sum_{i=1}^{3} s_{fi}\left(\dot{z}_{fi} + \dot{d}_i\right) \\
&= \sum_{i=1}^{3} s_{fi}\left(-k_1\lceil s_{fi}\rfloor^{q_1} - k_2\lceil s_{fi}\rfloor^{q_2} - k_3\lceil s_{fi}\rfloor^{0} + \dot{d}_i\right) \\
&= \sum_{i=1}^{3}\left(-k_1|s_{fi}|^{2r_3} - k_2|s_{fi}|^{2r_4} - k_3|s_{fi}| + \dot{d}_i s_{fi}\right) \\
&= \sum_{i=1}^{3}\left(-k_1|s_{fi}|^{2r_3} - k_2|s_{fi}|^{2r_4} - (k_3 - L)|s_{fi}|\right)
\end{aligned} \tag{42}$$

where $r_3 = 1/2 + q_1/2 \in (0, 1)$, $r_4 = 1/2 + q_2/2 \in (1, \infty)$.

Via Lemma 5, we have

$$\begin{aligned}
V_f^{r_3} &\leqslant \frac{1}{2^{r_3}}\sum_{i=1}^{3}\left(|s_{fi}|^{2r_3}\right) \\
V_f^{r_4} &\leqslant \frac{3^{r_4-1}}{2^{r_4}}\sum_{i=1}^{3}\left(|s_{fi}|^{2r_4}\right)
\end{aligned} \tag{43}$$

Also, note that $k_1, k_2 > 0$ and $k_3 > L$, then (42) and (43) implies that

$$\begin{aligned}
\dot{V}_f &\leqslant -k_1\sum_{i=1}^{3}\left(|s_{fi}|^{2r_3}\right) - k_2\sum_{i=1}^{3}\left(|s_{fi}|^{2r_4}\right) \\
&\leqslant -2^{r_3}k_1 V_f^{r_3} - \frac{2^{r_4}}{3^{r_4-1}}k_2 V_f^{r_4}
\end{aligned} \tag{44}$$

Therefore, according to Lemma 1, $\boldsymbol{s_f}$ converges to zero in fixed time, and the settling time T_2 is bounded by

$$\begin{aligned}
T_2 &\leqslant \frac{1}{2^{r_3}k_1(1-r_3)} + \frac{3^{r_4-1}}{2^{r_4}k_2(r_4-1)} \\
&= \frac{2}{2^{1/2+q_1/2}k_1(1-q_1)} + \frac{2\times 3^{q_2/2-1/2}}{2^{1/2+q_2/2}k_2(q_2-1)}
\end{aligned}$$

Hence, for $t \geqslant T_2$, when $\boldsymbol{s_f} = 0$, the attitude dynamics in sliding mode become $\dot{\boldsymbol{v}} = \dot{\boldsymbol{v}}_{\boldsymbol{n}} = -H(\boldsymbol{e})\boldsymbol{a}(\boldsymbol{e},\boldsymbol{\xi})$ via (36) and (37), which is the same as the nominal closed-loop system (8). Consequently, it follows from Lemma 7 that $\boldsymbol{e}$ and $\boldsymbol{v}$ converge to zero in fixed time $T_1 + T_2$. ■

Remark 3: From Eqns. (42) and (39), it can be seen that large k_1 and k_2 imply fast convergence rate in the reaching phase, and large k_3 means better disturbance attenuation performance. However, in practice, the value of controller gains are limited by the bandwidth and magnitude of actuators. Besides, too large k_3 may cause significant chattering induced by time delay or measurement noise. Therefore, compromises should be made when selecting k_1, k_2 and k_3.

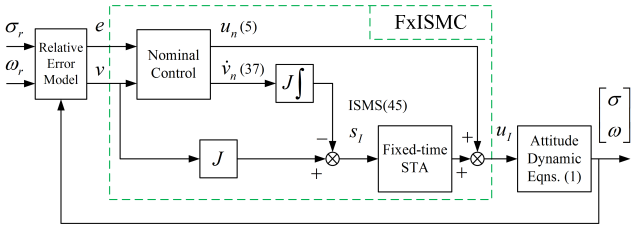

FIGURE 2. Block diagram of closed-loop attitude system with FxISMC.

Remark 4: The reason why the sliding mode surface (38) is called the FSMS is because the order of the open-loop attitude dynamics (1) is the same as that of the FSMS (36). Note that the relative angular acceleration $\dot{\boldsymbol{v}}$ is needed in (36) but usually unavailable in practice. One solution is to apply the fixed-time differentiator [35] to estimate $\dot{\boldsymbol{v}}$,

$$\begin{cases}
\dot{x}_i = -\gamma_1(\lceil z_i\rfloor^{\frac{1}{2}} + \mu\lceil z_i\rfloor^{\frac{3}{2}}) + y_i \\
\dot{y}_i = -\gamma_2(\frac{1}{2}\lceil z_i\rfloor^{0} + 2\mu z_i + \frac{3}{2}\mu^2\lceil z_i\rfloor^{2}) \quad (i = 1, 2, 3)
\end{cases} \tag{45}$$

where $z_i = x_i - v_i$, $\gamma_1 > 2\sqrt{L_v}$, $\gamma_2 > 2L_v$, $L_v = \max_{t>0}|\dot{v}_i|$. It is shown in [35] that x_i and y_i converge to v_i and $\dot{v}_i$ in fixed time, $i = 1, 2, 3$.

C. INTEGRAL SLIDING MODE CONTROLLER DESIGN

Although the fixed-time attitude tracking problem is solved by the full-order sliding mode controller (38), it is worth noting that $\dot{\boldsymbol{v}}$ or its estimation is required in FSMS (36), however $\dot{\boldsymbol{v}}$ is usually sensitive to the measurement noise. In this subsection, the integral sliding mode technique is adopted to design fixed-time integral sliding mode controller (FxISMC) without using $\dot{\boldsymbol{v}}$.

The block diagram of our proposed FxISMC is illustrated in Fig. 2, where the integral sliding mode surface (ISMS) $\boldsymbol{s_I}$ is designed as the the angular momentum tracking error,

$$\boldsymbol{s_I} = \boldsymbol{J}\boldsymbol{v} - \boldsymbol{J}\boldsymbol{v}_{\boldsymbol{n}} \tag{46}$$

where $\boldsymbol{v_n}$ is defined in (37), and fixed time STA technique [35] is adopted to realize second-order sliding mode $\boldsymbol{s_I} = \dot{\boldsymbol{s}}_{\boldsymbol{I}} = 0$. Note that $\boldsymbol{v_n}$ can be rewritten as

$$\boldsymbol{v_n} = \boldsymbol{v}(0) - \int_{\tau=0}^{t} H(\boldsymbol{e})\boldsymbol{a}(\boldsymbol{e},\boldsymbol{\xi})d\tau$$

Then, the integral sliding mode surface $\boldsymbol{s_I}$ is equivalent to

$$\boldsymbol{s_I} = J\boldsymbol{v} - J\boldsymbol{v}(0) + \boldsymbol{J}\int_{\tau=0}^{t} H(\boldsymbol{e})\boldsymbol{a}(\boldsymbol{e},\boldsymbol{\xi})d\tau \tag{47}$$

Noting that $\boldsymbol{s_I}$ can be regard as the integral of full-order sliding mode $\boldsymbol{s_f}$ in (36), hence when $\dot{\boldsymbol{s}}_{\boldsymbol{I}} = 0$, the attitude system is equivalent to the nominal closed-loop system (8). Base on the STA technique, the following integral sliding

mode controller $\boldsymbol{u_I}$ is proposed to realize the second-order sliding mode motion $\boldsymbol{s_I} = \boldsymbol{0}$ and $\dot{\boldsymbol{s}}_{\boldsymbol{I}} = \boldsymbol{0}$.

$$\begin{cases} \boldsymbol{u_I} = \boldsymbol{u_n} - k_4 \left(\lceil \boldsymbol{s_I} \rfloor^{1/2} + \rho \lceil \boldsymbol{s_I} \rfloor^{3/2} \right) - \boldsymbol{z_I} \\ \dot{\boldsymbol{z}}_{\boldsymbol{I}} = k_5 \left(\frac{1}{2} \lceil \boldsymbol{s_I} \rfloor^0 + 2\rho \boldsymbol{s_I} + \frac{3}{2} \rho^2 \lceil \boldsymbol{s_I} \rfloor^2 \right) \end{cases} \tag{48}$$

where $\boldsymbol{u_n}$ is the same as (5).

Theorem 2: For the spacecraft attitude control system in (1) with Assumptions 1 satisfied, suppose that the controller is designed as (48) and the sliding mode surface is designed as (47). If the control law parameters satisfy $k_4 > 2\sqrt{L}$, $k_2 > 2L$, $\mu > 0$, then the second-order sliding mode $\boldsymbol{s_f} = \dot{\boldsymbol{s}}_{\boldsymbol{f}} = \boldsymbol{0}$ will be established in fixed time, furthermore, attitude tracking errors $\boldsymbol{e}$ and $\boldsymbol{v}$ will converge to zero in fixed time.

Proof: Substituting (48) and (5) into (3), we have

$$\boldsymbol{J}\dot{\boldsymbol{v}} = -H(\boldsymbol{e})\boldsymbol{J}\boldsymbol{a}(\boldsymbol{e}, \boldsymbol{\xi}) - k_4 \left(\lceil \boldsymbol{s_I} \rfloor^{1/2} + \rho \lceil \boldsymbol{s_I} \rfloor^{3/2} \right) - \boldsymbol{z_I} + \boldsymbol{d}$$

Then, the derivative of $\boldsymbol{s_I}$ becomes

$$\begin{aligned} \dot{\boldsymbol{s}}_{\boldsymbol{I}} &= \boldsymbol{J}\dot{\boldsymbol{v}} - \boldsymbol{J}\dot{\boldsymbol{v}}_{\boldsymbol{n}} \\ &= -k_4 \left(\lceil \boldsymbol{s_I} \rfloor^{1/2} + \rho \lceil \boldsymbol{s_I} \rfloor^{3/2} \right) - \boldsymbol{z_I} + \boldsymbol{d} \end{aligned} \tag{49}$$

Define an auxiliary variable $\boldsymbol{w_I}$ as $\boldsymbol{w_I} = \boldsymbol{d} - \boldsymbol{z_I}$, then, the closed-loop sliding mode dynamics (49) and (48) can be transformed into

$$\begin{cases} \dot{\boldsymbol{s}}_{\boldsymbol{I}} = -k_4 \left(\lceil \boldsymbol{s_I} \rfloor^{1/2} + \rho \lceil \boldsymbol{s_I} \rfloor^{3/2} \right) + \boldsymbol{w_I} \\ \dot{\boldsymbol{w}}_{\boldsymbol{I}} = -k_5 \left(\frac{1}{2} \lceil \boldsymbol{s_I} \rfloor^0 + 2\rho \boldsymbol{s_I} + \frac{3}{2} \rho^2 \lceil \boldsymbol{s_I} \rfloor^2 \right) + \dot{\boldsymbol{d}} \end{cases} \tag{50}$$

It follows from Lemma 2 that $\boldsymbol{s_I}$ and $\boldsymbol{w_I}$ converge to zero in fixed time. Then, $\dot{\boldsymbol{s}}_{\boldsymbol{I}}$ also converges to zero in fixed time according to (50). Once the second order sliding mode is established, the attitude dynamics becomes the nominal closed-loop system (8), and $\boldsymbol{e}$ and $\boldsymbol{v}$ converge to zero in fixed time via Lemma 7.

■

Remark 5: It is worthy mention that $\dot{\boldsymbol{s}}_{\boldsymbol{I}} = \boldsymbol{0}$ is necessary in the proof, but most existing FxISMC results [27], [34] can only achieve first-order sliding mode $\boldsymbol{s_I} = \boldsymbol{0}$, and $\dot{\boldsymbol{s}}_{\boldsymbol{I}}$ is regarded as $\boldsymbol{0}$. However, $\dot{\boldsymbol{s}}_{\boldsymbol{I}} = \boldsymbol{0}$ can not necessarily be implied by $\boldsymbol{s_I} = \boldsymbol{0}$ directly, since $\dot{\boldsymbol{s}}$ is discontinuous or nonexistent [38]. To this end, the recently proposed fixed-time STA [35] is adopted here to achieves second-order sliding mode $\boldsymbol{s_I} = \boldsymbol{0}$ and $\dot{\boldsymbol{s}}_{\boldsymbol{I}} = \boldsymbol{0}$.

Remark 6: According to the analysis in [35], large k_4, k_5 would accelerate the sliding reaching phase and provide large tolerable range of disturbance. However, the estimate of settling time is very crude. Hence, as is recommended in [35], parameters k_4, k_5, and ρ can be selected via simulation.

Remark 7: Notice that adding a power integrator technique is also adopted in the recent work [31] to achieve a fixed-time attitude stabilization. Compared with the controller [31], our method provide a more explicit and direct relationship between the maximum settling time (9) and parameter condition (7). Moreover, different from [31], the proposed FxFSMC (38) and FxISMC (48) are both continuous, since the discontinuous term $\lceil \boldsymbol{s_f} \rfloor^0$ and $\lceil \boldsymbol{s_I} \rfloor^0$ are integrated in control laws $\boldsymbol{u_f}$ and $\boldsymbol{u_I}$. Hence the proposed controllers are chattering-free in theory. This feature is also suitable for practice, because the commonly used actuators, such as control moment gyroscopes and reaction wheel can only provide continuous control torques.

Remark 8: Different from the fixed-time sliding mode controllers based on feedback linearization or state transformation [24]–[27], our sliding mode surfaces are designed based on attitude and angular velocity explicitly and directly. Therefore, the proposed sliding mode surfaces (36) and (47) have a clearer physical meaning and reduce the computation burden caused by the accurate compensation terms and the inverse of the Jacobian matrix in [24]–[27].

Remark 9: Note that the bound of derivative disturbance L is required in our FxFSMC (38) and FxISMC (48). However, it is difficult to obtain this parameter when the flexible vibration or uncertainties in moments of inertia is considered. If the bound L is unknown, our recommendation is to utilize adaptive methods to estimate the bound of derivative disturbance.

Remark 10: Our proposed FxFSMC and FxISMC can be extended to the Rodrigues parameter directly, and to the quaternion and rotation matrix using feedback linearization.

IV. SIMULATION RESULTS

In this section, simulations results are presented to verify the effectiveness of the proposed controllers FxFSMC (38) and FxISMC (48) in various scenarios. The recent proposed finite-time integrate sliding mode controller (denoted by FnISMC) in [34] is used here for comparison purpose.

Consider the rigid spacecraft with the inertia matrix $\boldsymbol{J} = [20, 1.2, 0.9; 1.2, 17, 1.4; 0.9, 1.4, 15]\text{kg} \cdot \text{m}^2$ [1]. The external disturbances are $d = [1\sin(0.8t + 1), 1.5\sin(0.6t + 2), 2\sin(0.4t + 3)]^T \text{N} \cdot \text{m}$ satisfying Assumption 1 with $L = 1$. The initial MRPs of desired attitude and angular velocity are $\boldsymbol{\sigma_r}(0) = \boldsymbol{0}$ and $\boldsymbol{\omega_r}(0) = \boldsymbol{0}$, and the desired angular velocity is set as $\boldsymbol{\omega_r}(t) = [0.2\sin(0.3\,t), 0.3\sin(0.3\,t), 0.4\sin(0.4\,t)]$.

The parameters of FxFSMC and FxISMC are chosen via our recommended processes in Remark 2, 3, and 6, which are given as $c_1 = 0.81$, $c_2 = 1.45$, $\lambda_1 = 0.14$, $\lambda_2 = 0.15$, $\lambda_3 = 1.0$, $p = 0.8$, $q = 1.2$ ($\mu_1 = \mu_2 = 0.2$), $k_1 = 1.5$, $k_2 = 2$, $k_3 = 1$, $k_4 = k_5 = 2$, $\rho = 1$, . The parameters of FnISMC in [34] are determined by trial and error until a good tracking performance is achieved, and are given as $k_1 = 1$, $k_2 = 1$, $k_3 = 1.5$, $\alpha_1 = 0.9$. Note that the discontinuous sign function in FxFSMC [34] is approximated by the saturation function $s_i/(|s_i| + \Phi)$ with $\Phi = 0.001$ to reduce inevitable chattering induced by noises. The discontinuous terms $\lceil \cdot \rfloor^0$ in FxFSMC and FxISMC are directly utilized in simulation without any approximation.

A. COMPARATIVE SIMULATION WITH EXTERNAL DISTURBANCE

This subsection focuses on the disturbance attenuation performance analysis of FnISMC, FxFSMC, and FxISMC. The

TABLE 1. Comparation results without measurement noise and saturation.

Controller	ST	UB_e	UB_v	M_u
FnISMC	11.0	4.10×10^{-6}	1.14×10^{-5}	48.71
FxFSMC	8.31	8.79×10^{-9}	2.08×10^{-7}	2885
FxISMC	8.32	1.88×10^{-10}	2.24×10^{-7}	154.3

responses of state and control signals in the case of $\boldsymbol{\sigma}(0) = [0.5; -0.4; 0.3]^T$, $\boldsymbol{\omega}(0) = [-0.05; 0.04; -0.03]^T$ rad/s are presented in Figs. 3 - 5, and the performances are summarized in Table 1, where UB_e and UB_v denote the ultimate bounds (UB) on steady states of $\|\boldsymbol{e}\|$ and $\|\boldsymbol{v}\|$ respectively, ST denotes the settling time (time after which $\|e\| < 0.01$ and $\|v\| < 0.02$ hold), and $\mathrm{M}_u = \max_{t\geq 0, i=1,2,3} |u_i|$ denotes the maximum amplitude of control signals.

It can be seen from Figs. 3 - 4 that all the controllers can achieve finite-time state convergence of $\boldsymbol{e}, \boldsymbol{v}$. It follows from the logarithm curves of the absolute value $|e_i|$, $|v_i|$, $i = 1, 2, 3$ in the figures and the values of UB_e and UB_v in Table 1 that proposed FxFSMC and FxISMC have much better steady-state precision compared with the first-order FnISMC. Also, the chattering phenomenon is avoided for all controllers according to the curves of $\boldsymbol{u}$ in Fig. 5. However, it can be seen from M_u index in Table 1 that the fixed-time controllers FxFSMC and FxISMC require larger control magnitudes. It is also worth noting that the extremely large control in FxFSMC is caused by the initial estimate error of the fixed-time differentiator (45), hence FxISMC is more recommended if the angular acceleration is not measurable.

Moverover, the relationships between settling time and initial conditions are discussed here. The initial states are set as

$$\begin{aligned} \boldsymbol{\sigma}(0) &= 0.2n[0.5; -0.4; 0.3]^T, \\ \boldsymbol{\omega}(0) &= 0.2n[-0.05; 0.04; -0.03]^T, \quad n = 1, \cdots, 10. \end{aligned} \tag{51}$$

The performances of the settling time with FnISMC, FxFSMC, and FxISMC are shown in Fig. 6, where $N = \|\boldsymbol{\sigma}(0)\|^2 + \|\boldsymbol{\omega}(0)\|^2$. It can be seen that the settling times of FxFSMC and FxISMC barely increase with initial conditions when $N > 1$, compared with that of FnISMC, which demonstrates the fixed-time convergence property of our proposed controllers.

B. COMPARATIVE SIMULATION WITH DISTURBANCE, SATURATION, UNCERTAINTY AND NOISE

In this subsection, more real scenarios are considered to test the robustness of the controllers of FnISMC, FxFSMC, and FxISMC in the last section. In order to take the actuator saturation into consideration, the maximum control torque is limited by $\pm$30Nm as the physical constraints.

Moreover, uncertainty in inertia matrix is introduced as $\Delta\boldsymbol{J} = [2, 0.12, 0.09; 0.12, 1.7, 0.14; 0.09, 0.14, 1.5]\mathrm{kg} \cdot \mathrm{m}^2$. Besides, the measured signals are also taken into consideration. Define $\boldsymbol{e_m} = \boldsymbol{e} + n_e\boldsymbol{\zeta_e}$ and $\boldsymbol{v_m} = \boldsymbol{v} + n_v\boldsymbol{\zeta_v}$, where

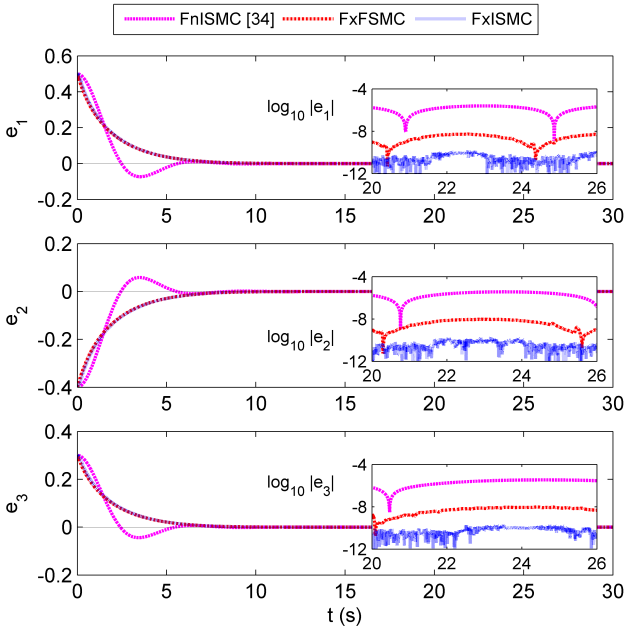

FIGURE 3. Attitude tracking errors $\boldsymbol{e}$ without measurement noise.

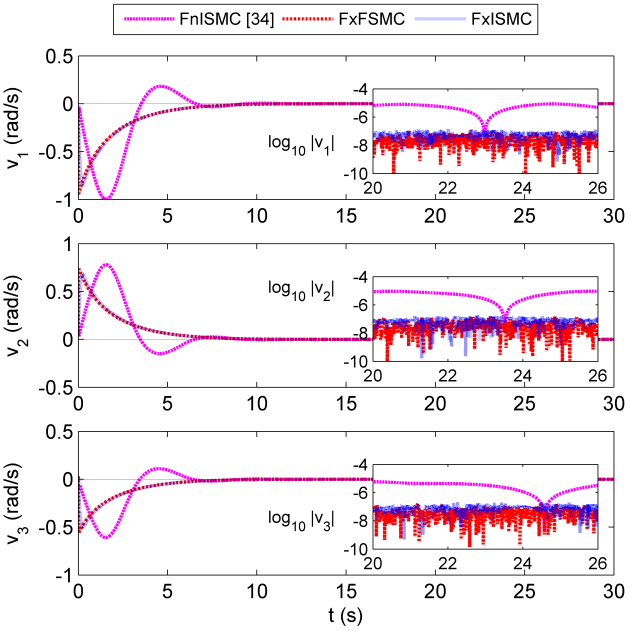

FIGURE 4. Angular velocities tracking errors $\boldsymbol{v}$ without measurement noise.

$\boldsymbol{\zeta_e} = [\zeta_{e1}, \zeta_{e2}, \zeta_{e3}]^T$ and $\boldsymbol{\zeta_v} = [\zeta_{v1}, \zeta_{v2}, \zeta_{v3}]^T$ are random variables with $\zeta_{ij} \in [-1, 1]$, $(i = e, v; j = 1, 2, 3)$, and $n_e = n_v = 0.01$ are the noise magnitudes. The raw measured signals $\boldsymbol{e_m}$ and $\boldsymbol{v_m}$ are filtered by a low-pass filter $1/(1+0.1s)$, where s is the Laplace variable.

The simulation results in the case of $\boldsymbol{\sigma}(0) = [0.5; -0.4; 0.3]^T$, $\boldsymbol{\omega}(0) = [-0.05; 0.04; -0.03]^T$ rad/s are given in Figs. 7 -9. The performance of the different controller

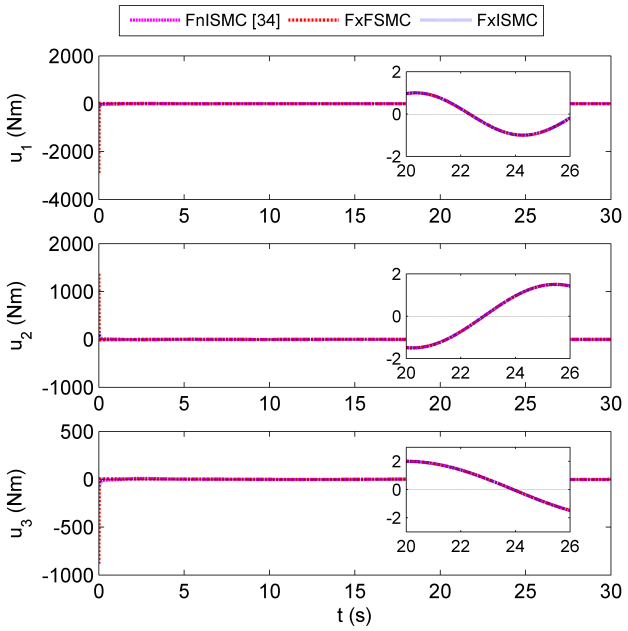

FIGURE 5. Control torques *u* without measurement noise.

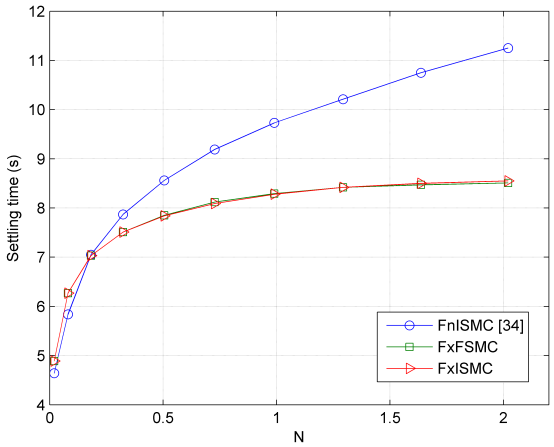

FIGURE 6. Settling time under different initial conditions without measurement noise.

TABLE 2. Comparation results with measurement noise and saturation.

Controller	ST	UB_e	UB_v
FnISMC	11.1	8.97×10^{-4}	7.40×10^{-3}
FxFSMC	8.63	2.68×10^{-4}	3.72×10^{-3}
FxISMC	8.62	3.23×10^{-4}	3.87×10^{-3}

is summarized in Table 2. Also, the settling time results for different initial conditions (51) are given in Fig. 10.

From Figs. 7 - 8 and Table 2, it can be seen that all controllers can resist the actuator saturation, and the proposed FxFSMC and FxISMC can achieve better steady precision than FnISMC, implying better robustness against disturbance and uncertainty in the presence of measurement noise.

Moreover, Fig. 10 shows that FxFSMC and FxISMC still guarantee faster convergence performance for large initial conditions even in the presence of actuator saturation.

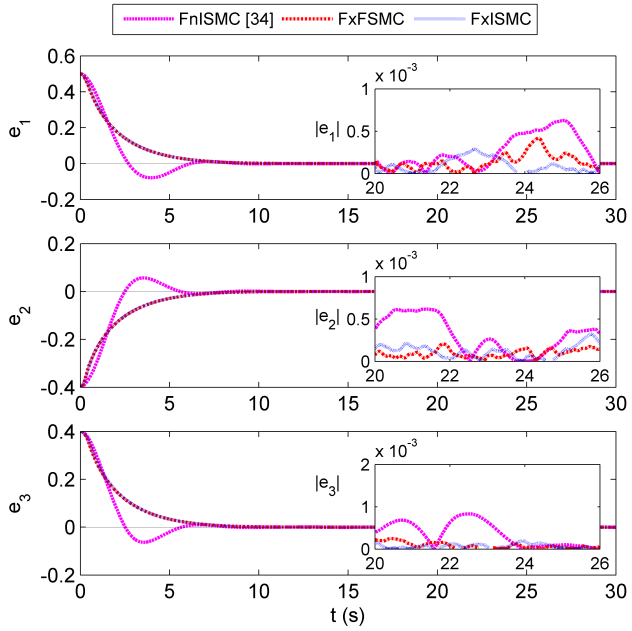

FIGURE 7. Attitude tracking errors *e* with saturation, noise, and uncertainty.

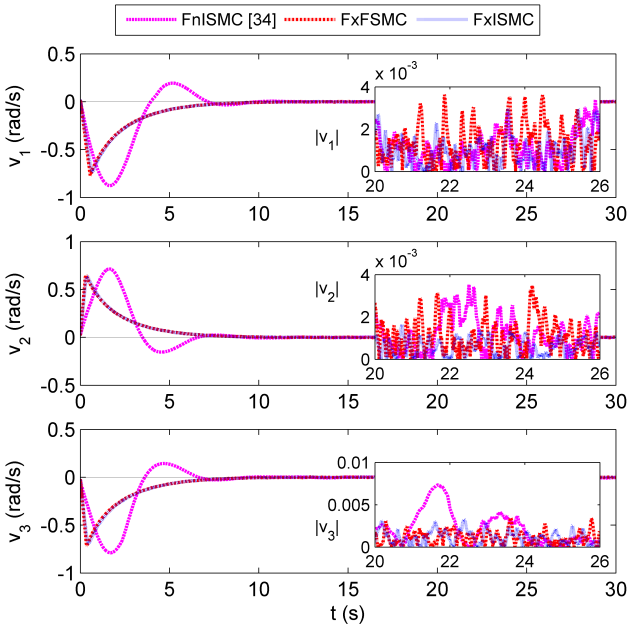

FIGURE 8. Angular velocities tracking errors *v* with saturation, noise, uncertainty.

It's noteworthy that the chattering phenomenon is excited by the measurement noise for the three controllers, while their chattering levels are basically in the same magnitude. These results coincide with theory, because the discontinuous switching terms are applied to the derivative of control signals in FxFSMC and FxISMC, they achieve similar chattering attenuation performance with FnISMC using saturation function.

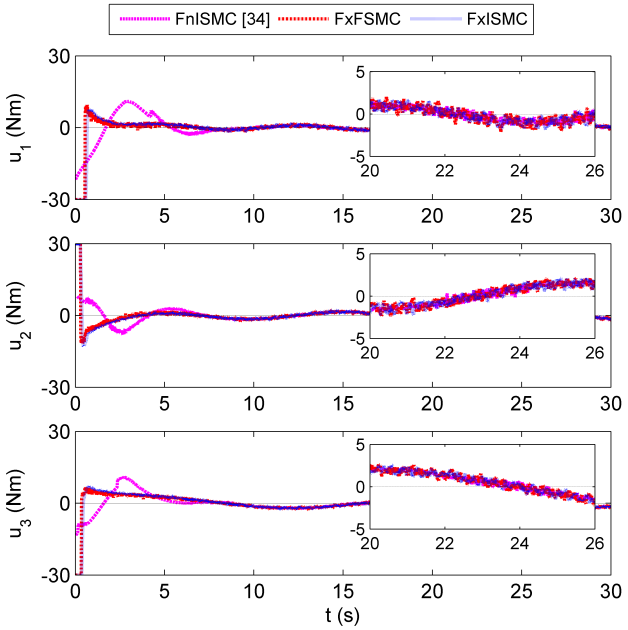

FIGURE 9. Control torques u with saturation, noise, and uncertainty.

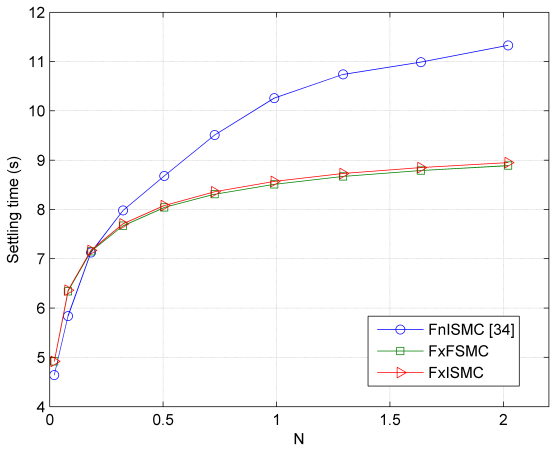

FIGURE 10. Settling time under different initial conditions with saturation, noise, and uncertainty.

V. CONCLUSION

In this paper, a fixed-time full-order sliding mode controller (FxFSMC) and a fixed-time integral sliding mode controller (FxISMC) are proposed to solve the fast and high-precision attitude tracking problem for the rigid spacecraft with unknown external disturbances. Firstly, via improving adding power integral techniques, the undisturbed nonlinear attitude tracking problem is addressed by the proposed nominal nonsingular fixed-time attitude controller without causing singularity. Based on this, a fixed-time full-order sliding mode controller is then proposed to handle the unknown external disturbances. Then, by utilizing integral sliding mode and STA technique, an integral sliding mode attitude controller is further proposed to eliminate the requirement of acceleration information in the full-order sliding mode controller. Compared with the existing results, the two proposed sliding mode controllers can provide strict fixed-time stability in both the reaching phase and the sliding phase. Moreover, the proposed controllers are also chattering-free and singular-free inherently. Finally, they can make the attitude tracing error converge to zero instead of a region in fixed time. Further work includes extending the results to the $SO(3)$ representation and flexible spacecraft.

APPENDIX
THE CHARACTERISTICS OF LYAPUNOV FUNCTION IN (14)

Lemma 8: Consider the function $V : \mathbb{R} \times \mathbb{R} \to \mathbb{R}$ with $p \in (0, 1)$

$$V(b,a) = \int_{x=a}^{b} \lceil x \rfloor^{1/p} - \lceil a \rfloor^{1/p} \mathrm{d}x$$

Then, we have

(1) $V(b, a) \geq 0$, the equality holds if and only if $a = b$.

(2) $V(b, a) \to +\infty$, as $|b - a| \to \infty$.

Proof: **(1)** Since $p/(1+p)\mathrm{d}|x|^{1+1/p} = |x|^{p-1}x\mathrm{d}x = \lceil x \rfloor^{1/p}\mathrm{d}x$, we have

$$\begin{aligned} V(b,a) &= \frac{p}{1+p}|b|^{1+\frac{1}{p}} - \frac{p}{1+p}|a|^{1+\frac{1}{p}} + \lceil a \rfloor^{\frac{1}{p}}(b-a) \\ &= \frac{p}{1+p}|b|^{1+\frac{1}{p}} + \frac{1}{1+p}|a|^{1+\frac{1}{p}} - \lceil a \rfloor^{\frac{1}{p}} b \\ &\geq \frac{p}{1+p}|b|^{1+\frac{1}{p}} + \frac{1}{1+p}|a|^{1+\frac{1}{p}} - |a|^{\frac{1}{p}}|b| \end{aligned}$$

where the equality holds if and only if $ab \geq 0$. Then, via Lemma 4, it follows that $V(b,a) \geq |a|^{\frac{1}{p}}|b| - |a|^{\frac{1}{p}}|b| = 0$, where the equality holds if and only if $|a| = |b|$. Hence, $V(b, a) \geq 0$, the equality holds if and only if $a = b$.

(2) Let $\{a_n\}$ and $\{b_n\}$ be arbitrary series that satisfy $\lim_{n\to\infty} |b_n - a_n| = \infty$. Define $V_n = V(b_n, a_n)$.

If $\lim_{n\to\infty} b_n - a_n = +\infty$, then $\forall \epsilon > 0$, $\exists N$ such that $b_n - a_n > \epsilon$ holds $\forall n > N$. It follows from Lemma 3 that

$$\begin{aligned} V_n &\geq \int_{x=a_n+\epsilon}^{b_n} \lceil x \rfloor^{1/p} - \lceil a_n \rfloor^{1/p} \mathrm{d}x \\ &\geq \int_{x=a_n+\epsilon}^{b_n} 2^{1-1/p}|x-a_n|^{1/p}\mathrm{d}x \\ &> 2^{1-1/p}\epsilon^{1/p}|b_n - a_n - \epsilon|, \quad \forall n > N. \end{aligned}$$

Hence, $\lim_{n\to\infty} V_n = +\infty$.

If $\lim_{n\to\infty} a_n - b_n = +\infty$, note that

$$V_n = \int_{x=b_n}^{a_n} \lceil a_n \rfloor^{1/p} - \lceil x \rfloor^{1/p} \mathrm{d}x$$

The rest of the proof is similar to the first case and hence is omitted here.

REFERENCES

[1] K. Lu and Y. Xia, "Adaptive attitude tracking control for rigid spacecraft with finite-time convergence," *Automatica*, vol. 49, no. 12, pp. 3591–3599, Dec. 2013.

[2] H. Du, S. Li, and C. Qian, "Finite-time attitude tracking control of spacecraft with application to attitude synchronization," *IEEE Trans. Autom. Control*, vol. 56, no. 11, pp. 2711–2717, Nov. 2011.

[3] B. Xiao, Q. Hu, and Y. Zhang, "Adaptive sliding mode fault tolerant attitude tracking control for flexible spacecraft under actuator saturation," *IEEE Trans. Control Syst. Technol.*, vol. 20, no. 6, pp. 1605–1612, Nov. 2012.

[4] H. Wong, M. S. de Queiroz, and V. Kapila, "Adaptive tracking control using synthesized velocity from attitude measurements," *Automatica*, vol. 37, no. 6, pp. 947–953, Jun. 2001. [Online]. Available: http://www.sciencedirect.com/science/article/pii/S0005109801000383
[5] S. Li, S. Ding, and Q. Li, "Global set stabilisation of the spacecraft attitude using finite-time control technique," *Int. J. Control*, vol. 82, no. 5, pp. 822–836, May 2009, doi: 10.1080/00207170802342818.
[6] F. Lizarralde and J. T. Wen, "Attitude control without angular velocity measurement: A passivity approach," *IEEE Trans. Autom. Control*, vol. 41, no. 3, pp. 468–472, Mar. 1996.
[7] J. T.-Y. Wen and K. Kreutz-Delgado, "The attitude control problem," *IEEE Trans. Autom. Control*, vol. 36, no. 10, pp. 1148–1162, Oct. 1991.
[8] N. A. Chaturvedi, A. K. Sanyal, and N. H. McClamroch, "Rigid-body attitude control," *IEEE Control Syst. Mag.*, vol. 31, no. 3, pp. 30–51, Jun. 2011.
[9] Z. Chen and J. Huang, "Attitude tracking and disturbance rejection of rigid spacecraft by adaptive control," *IEEE Trans. Autom. Control*, vol. 54, no. 3, pp. 600–605, Mar. 2009.
[10] S. R. Vadali, "Variable-structure control of spacecraft large-angle maneuvers," *J. Guid., Control, Dyn.*, vol. 9, no. 2, pp. 235–239, Mar. 1986.
[11] Z. Zhu, Y. Xia, and M. Fu, "Adaptive sliding mode control for attitude stabilization with actuator saturation," *IEEE Trans. Ind. Electron.*, vol. 58, no. 10, pp. 4898–4907, Oct. 2011.
[12] B. Cong, X. Liu, and Z. Chen, "Backstepping based adaptive sliding mode control for spacecraft attitude maneuvers," *Aerosp. Sci. Technol.*, vol. 30, no. 1, pp. 1–7, Oct. 2013. [Online]. Available: http://www.sciencedirect.com/science/article/pii/S1270963813001107
[13] E. Jin and Z. Sun, "Robust controllers design with finite time convergence for rigid spacecraft attitude tracking control," *Aerosp. Sci. Technol.*, vol. 12, no. 4, pp. 324–330, Jun. 2008.
[14] A. A. Zhang, B. C. Lv, C. Z. Zhang, and D. Z. She, "Finite time fault tolerant attitude control-based observer for a rigid satellite subject to thruster faults," *IEEE Access*, vol. 5, pp. 16808–16817, 2017.
[15] A.-G. Wu, R.-Q. Dong, Y. Zhang, and L. He, "Adaptive sliding mode control laws for attitude stabilization of flexible spacecraft with inertia uncertainty," *IEEE Access*, vol. 7, pp. 7159–7175, 2019.
[16] S. Ding and S. Li, "Stabilization of the attitude of a rigid spacecraft with external disturbances using finite-time control techniques," *Aerosp. Sci. Technol.*, vol. 13, nos. 4–5, pp. 256–265, Jun. 2009.
[17] Q. Hu and B. Jiang, "Continuous finite-time attitude control for rigid spacecraft based on angular velocity observer," *IEEE Trans. Aerosp. Electron. Syst.*, vol. 54, no. 3, pp. 1082–1092, Jun. 2018.
[18] C. Jing, H. Xu, X. Niu, and X. Song, "Adaptive nonsingular terminal sliding mode control for attitude tracking of spacecraft with actuator faults," *IEEE Access*, vol. 7, pp. 31485–31493, 2019.
[19] A.-M. Zou, K. D. Kumar, Z.-G. Hou, and X. Liu, "Finite-time attitude tracking control for spacecraft using terminal sliding mode and chebyshev neural network," *IEEE Trans. Syst. Man, Cybern. B, Cybern.*, vol. 41, no. 4, pp. 950–963, Aug. 2011.
[20] L. Zhao and Y. Jia, "Finite-time attitude tracking control for a rigid spacecraft using time-varying terminal sliding mode techniques," *Int. J. Control*, vol. 88, no. 6, pp. 1150–1162, Jun. 2015, doi: 10.1080/00207179.2014.996854.
[21] S. Shao, Q. Zong, B. Tian, and F. Wang, "Finite-time sliding mode attitude control for rigid spacecraft without angular velocity measurement," *J. Franklin Inst.*, vol. 354, no. 12, pp. 4656–4674, Aug. 2017.
[22] A. Polyakov, "Nonlinear feedback design for fixed-time stabilization of linear control systems," *IEEE Trans. Autom. Control*, vol. 57, no. 8, pp. 2106–2110, Aug. 2012.
[23] B. Jiang, Q. Hu, and M. I. Friswell, "Fixed-time attitude control for rigid spacecraft with actuator saturation and faults," *IEEE Trans. Control Syst. Technol.*, vol. 24, no. 5, pp. 1892–1898, Sep. 2016.
[24] B. Huang, A.-J. Li, Y. Guo, and C.-Q. Wang, "Fixed-time attitude tracking control for spacecraft without unwinding," *Acta Astronautica*, vol. 151, pp. 818–827, Oct. 2018. [Online]. Available: http://www.sciencedirect.com/science/article/pii/S0094576518301589
[25] X.-N. Shi, Y.-A. Zhang, D. Zhou, and Z.-G. Zhou, "Global fixed-time attitude tracking control for the rigid spacecraft with actuator saturation and faults," *Acta Astronautica*, vol. 155, pp. 325–333, Feb. 2019. [Online]. Available: http://www.sciencedirect.com/science/article/pii/S0094576517305210
[26] C. Ton and C. Petersen, "Continuous fixed-time sliding mode control for spacecraft with flexible appendages," *IFAC-PapersOnLine*, vol. 51, no. 12, pp. 1–5, 2018. [Online]. Available: http://www.sciencedirect.com/science/article/pii/S240589631830822X
[27] J. Gao, Z. Fu, and S. Zhang, "Adaptive fixed-time attitude tracking control for rigid spacecraft with actuator faults," *IEEE Trans. Ind. Electron.*, vol. 66, no. 9, pp. 7141–7149, Sep. 2019.
[28] Y. Huang and Y. Jia, "Robust adaptive fixed-time tracking control of 6-DOF spacecraft fly-around mission for noncooperative target," *Int. J. Robust Nonlinear Control*, vol. 28, no. 6, pp. 2598–2618, Apr. 2018. [Online]. Available: https://onlinelibrary.wiley.com/doi/abs/10.1002/rnc.4038
[29] Q. Chen, S. Xie, M. Sun, and X. He, "Adaptive nonsingular fixed-time attitude stabilization of uncertain spacecraft," *IEEE Trans. Aerosp. Electron. Syst.*, vol. 54, no. 6, pp. 2937–2950, Dec. 2018.
[30] J. Gao, S. Zhang, and Z. Fu, "Fixed-time attitude tracking control for rigid spacecraft with actuator misalignments and faults," *IEEE Access*, vol. 7, pp. 15696–15705, 2019.
[31] H. Du, J. Zhang, D. Wu, W. Zhu, H. Li, and Z. Chu, "Fixed-time attitude stabilization for a rigid spacecraft," *ISA Trans.*, vol. 98, pp. 263–270, Mar. 2020. [Online]. Available: http:/www.sciencedirect.com/science/article/pii/S0019057819303623
[32] Z. Song, C. Duan, H. Su, and J. Hu, "Full-order sliding mode control for finite-time attitude tracking of rigid spacecraft," *IET Control Theory Appl.*, vol. 12, no. 8, pp. 1086–1094, May 2018.
[33] P. M. Tiwari, S. Janardhanan, and M. un Nabi, "Attitude control using higher order sliding mode," *Aerosp. Sci. Technol.*, vol. 54, pp. 108–113, Jul. 2016.
[34] Y. Guo, B. Huang, S.-M. Song, A.-J. Li, and C.-Q. Wang, "Robust saturated finite-time attitude control for spacecraft using integral sliding mode," *J. Guid., Control, Dyn.*, vol. 42, no. 2, pp. 440–446, Feb. 2019.
[35] E. Cruz-Zavala, J. A. Moreno, and L. M. Fridman, "Uniform robust exact differentiator," *IEEE Trans. Autom. Control*, vol. 56, no. 11, pp. 2727–2733, Nov. 2011.
[36] S. Ding, S. Li, and W. X. Zheng, "Nonsmooth stabilization of a class of nonlinear cascaded systems," *Automatica*, vol. 48, no. 10, pp. 2597–2606, Oct. 2012. [Online]. Available: http://www.sciencedirect.com/science/article/pii/S0005109812003263
[37] A.-M. Zou, A. H. J. de Ruiter, and K. D. Kumar, "Distributed finite-time velocity-free attitude coordination control for spacecraft formations," *Automatica*, vol. 67, pp. 46–53, May 2016. [Online]. Available: http://www.sciencedirect.com/science/article/pii/S0005109815005610
[38] A. Levant, "Principles of 2-sliding mode design," *Automatica*, vol. 43, no. 4, pp. 576–586, Apr. 2007.

LEI WANG was born in Hunan, China, in 1991. He received the B.S. degree from the School of Aerospace engineering, Beijing Institute of Technology, Beijing, China, in 2013. He is currently pursuing the Ph.D. degree with the School of automation, Beijing Institute of Technology, where he works on non-linear robust control, intelligent complex system, spacecraft, and aircraft control technology and applications.

ZHUOYUE SONG received the B.S. degree in electrical engineering and automation from the Hebei University of Science and Technology, in 2004, the M.S. degree (Hons.) in control science and engineering from the Harbin University of Technology, in 2007, and the Ph.D. degree in electrical and electronic engineering from The University of Manchester, in 2011. She is currently an Associate Professor with the School of Automation, Beijing Institute of Technology, Beijing, China. Her research interests include analysis and synthesis for control systems, with particular attention to uncertainty, optimization, and multi-agent systems.